Journal of Food Engineering 109 (2012) 22–31

Contents lists available at SciVerse ScienceDirect

Journal of Food Engineering

journal homepage: www.elsevier.com/locate/jfoodeng

Optimization of operating conditions of a cooling tunnel for production of hard candies

María Agustina Reinheimer [a,*], Sergio F. Mussati [a,b], Nicolás J. Scenna [a,b]

[a] CAIMI – Centro de Aplicaciones Informáticas y Modelado en Ingeniería-UTN, FRRo – Universidad Tecnológica Nacional, Facultad Regional Rosario, Zeballos 1346, S2000BQA Rosario, Argentina

[b] INGAR-CONICET, Instituto de Desarrollo y Diseño, Avellaneda 3657, S3002GJC Santa Fe, Argentina

ARTICLE INFO

Article history:
Received 23 May 2011
Received in revised form 13 September 2011
Accepted 8 October 2011
Available online 15 October 2011

Keywords:
Hard candy
Cooling process
Optimization

ABSTRACT

On large industrial scales, the cooling stage in the production process of hard candies is one of the most critical unit operations because many quality problems such as deformation, fragility and aggregation may appear in this stage. Therefore, the optimization of the operating conditions of the cooling tunnel plays an essential role from a quality point of view.

The objective of this work is to develop a mathematical model to determine the optimal operating conditions of the cooling tunnel in order to assure the product quality. The resulting PDAEs were converted to a set of nonlinear algebraic equations using the centered finite difference approximation (CFDM) and were implemented into the optimization environment GAMS (General Algebraic Modeling System). Thus, the temperature profiles in the center and surface of the candy, air cooling temperature and velocity are simultaneously optimized. Three objectives functions based on the product quality are proposed. A sensitive analysis on the main model parameters was also made. The obtained results are discussed in detail. It is concluded that the developed model can be used as a useful tool to improve its operating efficiency and even to design a new cooling tunnel.

1. Introduction

The design and optimization of thermal processing of foods need accurate dynamic models through which systematically explore sets of highly nonlinear partial differential equations (PDEs), which are difficult and costly to solve, especially in terms of computation time (Balsa-Canto et al., 2002).

Current state in food science and technology databases reveals that many efforts have been made in the simulation and optimization of process unit operations (Barttfeld et al., 2006; Espinoza-Pérez et al., 2007; Nowee et al., 2007; Norton et al., 2009; Kiziltaş et al., 2010; Purlis, 2011).

Optimization using response surface modeling (RSM) has been the most common approach (Bouraoui et al., 1998; Erbar and Icier, 2009; Firatligil-Durmus and Evranuz, 2010) applied in food processing sector. RSM techniques were introduced in the 1950s associated with design of experiments methods (Box et al., 1978; Myers and Montgomery, 2002). In these statistical techniques, very simple empirical models are derived from sets of RSM experiments.

Though a number of robust optimization techniques have been successfully applied to solve several problems in the area of process engineering, little work is done in order to build powerful mathematical tools for decision support systems and optimization in the field of food processing sector (Banga et al., 2003).

There are several powerful solvers for NLP models (CONOPT, IPOPT, MINOS) which can be linked to different mathematical programming languages (GAMS, AMPL, AIMMS) in order to exploit their advantages in the food processing area.

With regards to the production line of hard candies, one of the most critical unit operations is the cooling of candies because many problems affecting the final product quality may appear if the cooling tunnel does not operate efficiently. Certainly, the main problems affecting hard candies' final quality are:

- Deformation due to excessive temperature at the tunnel exit. This incident is associated with the non-uniform radial temperature profiles of hard candies during cooling.
- Fragility to undergo the subsequent wrapping step because of sharp cooling. This phenomenon is observed when the operating conditions of the tunnel are high air velocity and low air temperature. Under these conditions, the surfaces of hard candies are cooled too fast becoming easily broken.
- Aggregation of candies due to inadequate residence time of candy inside the tunnel.

The samples which exhibit one of these problems are considered as non-conforming products and must be reprocessed.

* Corresponding author. Tel.: +54 341 4480102; fax: +54 341 4553439.
E-mail addresses: mareinheimer@santafe-conicet.gov.ar, magu_reinheimer@hotmail.com (M.A. Reinheimer).

0260-8774/$ - see front matter © 2011 Elsevier Ltd. All rights reserved.
doi:10.1016/j.jfoodeng.2011.10.009

Nomenclature

A	heat transfer area (m^2)
C_p	specific heat capacity (J/kg °C)
D	sample diameter (m)
G_1, G_1	air mass flow rate (kg/s)
h	heat transfer coefficient (W/m^2 °C)
H	enthalpy (J/kg)
H_{CW}	enthalpy computed at T_{CW} (J/kg)
H_{HW}	enthalpy computed at T_{HW} (J/kg)
H_{HE}	enthalpy computed at T_{HE} (J/kg)
k	thermal conductivity (W/m °C)
L	water mass flow rate (kg/s)
M	number of radial discretization points
N	number of temporal discretization points
q	heat transfer rate (W)
R	sample radius (m)
r	variable radius (m)
Rec	recycle air mass flow rate (kg/s)
RH	relative humidity (%)
S	air duct cross section (m^2)
$T(i,j)$	temperature in each discretization node "i, j" (°C)
T_{CW}	cooling water temperature (°C)
T_{HW}	heating water temperature (°C)
T_{HE}	air stream temperature at heat exchanger (°C)
T_a	cooling air temperature (°C)
T_{ref}	reference temperature (273.15 K)
ΔT	temperature variation (°C)
ΔT_{lm}	logarithmic mean temperature difference (°C)
t	time (s)
Δt	temporal grid with (m)
U	overall heat transfer coefficient (W/m^2 °C)
v_a	cooling air velocity (m/s)
Y	recycle ratio

Dimensionless numbers

Nu	Nusselt
Pr	Prandtl
Re	Reynolds

Greek symbols

α	thermal diffusivity (m^2/s)
δ	spatial grid with (m)
ρ	density (kg/m^3)
μ	viscosity (N s/m^2)
θ	residence time (s)

Subscripts

a	cooling air
amb	ambient air
c	candy
CW	cold water utility
HW	hot water utility
HE	heat exchanger
i	spatial node index
j	temporal node index
T	tunnel
W	water stream

Superscripts

inl	inlet
out	outlet

The objective of this work is to develop a dynamic mathematical model for the simultaneous optimization of operating conditions of the cooling tunnel in order to preserve the product quality. For the modeling purpose, the set of partial differential equations (PDEs) is discretized using the central finite difference method (CFDM), leading to a nonlinear programming model (NLP).

The paper is organized as follows. Section 2 briefly describes the production line of hard candies. Section 3 deals with the problem statement. Section 4 lists the assumptions and presents the mathematical model. Section 5 describes experimental procedure for temperature measurements. Section 6 presents applications of the developed NLP model and the discussion of results. Finally, Section 7 presents the conclusions and future work.

2. Production process of hard candy

Fig. 1 schematically shows the required unit operations for hard candy production process.

During the manufacturing process, granulated sugar, glucose and water are heated in a steam heated vessel for the sugar to be dissolved and then transferred to a batch vacuum cooker and boiled to remove almost all water. Thus the syrup with 19% of humidity is turned into a candy dough with 2.5% of humidity. The cooker consists of flash and vacuum chambers. Here, cooking temperatures are higher than 140 °C at atmospheric pressure. Then the cooker pressure is modified by applying a vacuum of at least 700 mmHg during the last few minutes of the evaporation process in order to drive off excessive water and provide the hard candy with the desired humidity. The last cooking stage is the addition and mix of additives (acids, flavoring and coloring agents).

The next step is the dough tempering, where the candy mass is driven to a tempering stainless steel belt which is water refrigerated and then it is mixed to homogenize its temperature. After that, the "forming" process is achieved. The hard candy at 85 °C is shaped by cutting up a dough roll in a stamp-forming one-process. The formed hard candies are then cooled in a conventional cooling tunnel. Finally, hard candies are individually wrapped.

2.1. Description of cooling tunnel

Fig. 2 illustrates the cooling tunnel. The tunnel has two air ducts (entrance and exit). As shown in Fig. 1, the tunnel is composed of three conveyor belts (CB) which are mechanically driven by an engine connected to an adjustable frequency drive (AFD) to vary the residence time of candies.

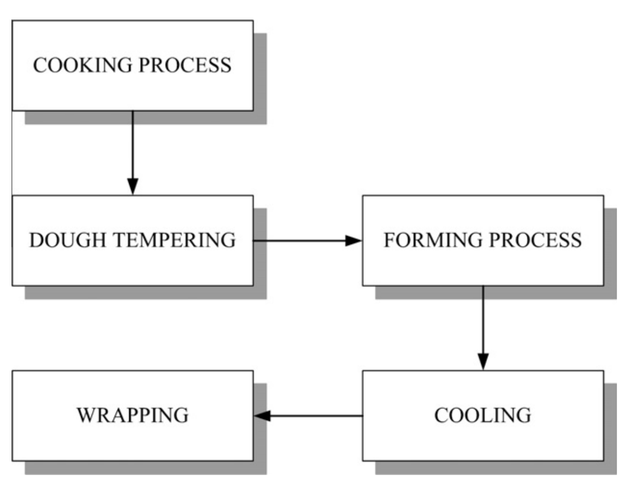

Fig. 1. Basic production process of hard candies.

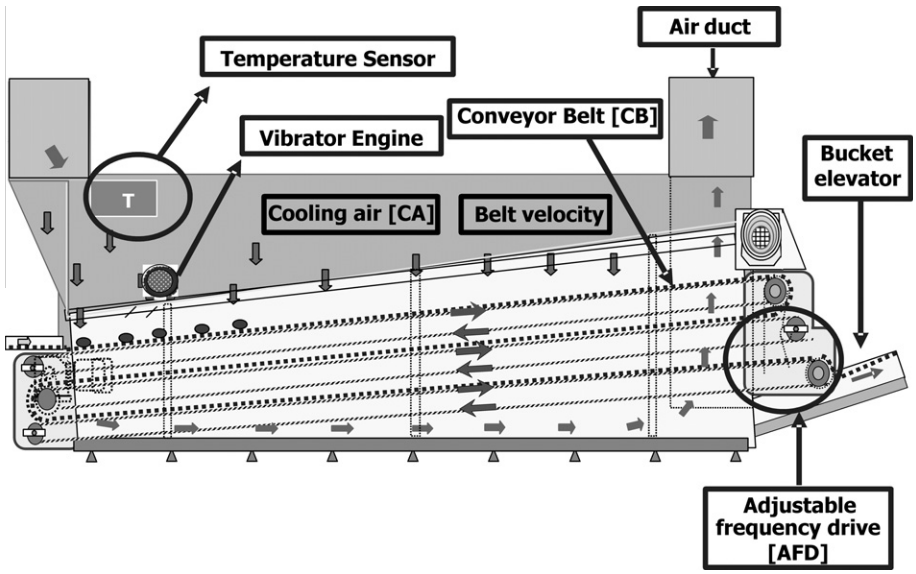

Fig. 2. A schematic cross-section of the cooling tunnel.

2.2. Air conditioning system: Operating policies

As mentioned before, the optimization model will lead the optimal values of the cooling air velocity and temperature to operate the tunnel. Also, it is necessary to air-condition the cooling stream in order to reach the optimal internal temperature distribution of hard candies. Air cooling velocity is easily regulated manipulating the operating speed range of the fan. On the other hand, the air cooling temperature is set up in a heat exchanger (HE) using auxiliary utilities (cooling/heating), as shown Fig. 3. The operating conditions of the heat exchanger depend on the external ambient temperature, and also this temperature depends on the season as well as the optimal value of the cooling temperature (Ta_T).

Thus, the cold water stream (CW) from the cooling tower may be used to cool the incoming air stream. Otherwise, in case that it is necessary to heat the air flow, hot water stream (HW), which is also used at the tempering stage to temper a stretch of the stainless steel belt, is available. Another available alternative for the stream which enters to the heat exchanger is to mix (M1) both mentioned utilities into a new stream (L_W).

As shown in Fig. 3 an alternative air recycle stream at the exit's duct is also included in the air conditioning system, increasing in this way, the available degrees of freedom in order to conveniently adjust the operating variables (fluxes and temperatures).

Summarizing, it is necessary to define a operational policy to adjust the air properties of the cooling stream (air velocity and temperature) by manipulating the fan velocity, the recycle stream and the stream fluxes in the heat exchanger (in case if needed).

Due to the fact that the way of operating the air conditioning system depends on the values of the optimal cooling air temperature inside the tunnel, Ta_T, and the ambient air temperature, T_{amb}, different alternatives are proposed, as is described below:

- If optimal $Ta_T < T_{amb}$, the cold water stream from the cooling tower (CT) will be used.
- If optimal $Ta_T = T_{amb}$ the way of operating is only using fresh air flow. Therefore the air-conditioning circuit will not put in operation. The model has the option to use or not the recycle flow (Rec).
- If optimal $Ta_T > T_{amb}$, the model has the option to mix or not the cold and hot water streams in the mixer M1.

3. Problem statement

The main aim of this paper is to optimize the operating conditions of the cooling stage in the production process of hard candies. More specifically, the goal is to develop a nonlinear programing (NLP) model in order to optimize simultaneously the unsteady

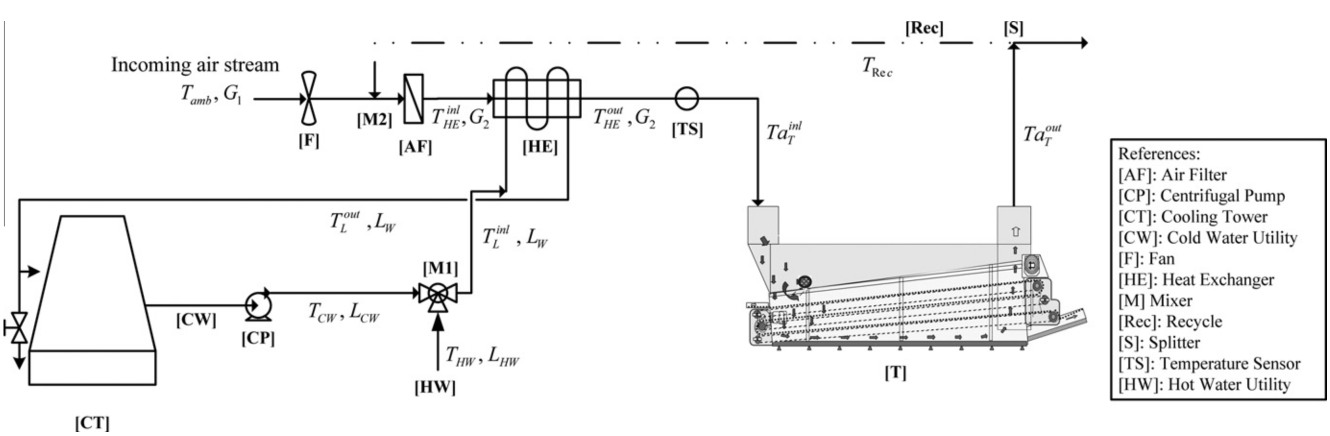

Fig. 3. Flow sheet of the integrated process (air conditioning process coupled with the cooling tunnel).

temperature distribution inside candies and temperature, velocities and flow-rate of air cooling to operate the cooling tunnel. In addition, the proposed model also includes the option of coupling the cooling stage with the air cooling conditioning process, and in this way, it allows the optimization of the integrated process. The variables for the air conditioning process are the flow-rates and temperatures of cold and hot streams used for heating and/or cooling (utilities).

Candy size and composition, ambient air temperature, heat transfer area and residence time of the candy inside the cooling tunnel are the main input data of the optimization model. Certainly, the heat transfer area of (HE), A, and the air duct section in the cooling tunnel, S, are assumed as given and known because these pieces of equipment already exist.

As will be more fully described in Section 4.2, several performance criteria related to the product quality are proposed as objective functions.

4. Assumptions and mathematical model

4.1. Assumptions

The main model assumptions can be summarized as follows:

- Candies are considered as homogeneous and isotropic spheres.
- Model 1-D. Temporal variations of the temperature in the radial direction are contemplated.
- Choi and Okos models (Choi and Okos, 1986) were used for thermo-physical property estimations, such as density, thermal capacity and thermal conductivity.
- Thermo-physical property variations with the temperature are neglected for the temperature range considered in this work.
- There is no moisture loss. Due to the low water content of hard candy (2.5%), water loss hardly occurs during candies cooling. According to this, moisture intake from air is also negligible, due to the fact that air humidity was monitored and profiles could be considered as constant between the values at tunnel entrance and exit.
- Changes in air temperature and humidity are small enough to produce a negligible effect on the thermal-physical properties of the air. Based on this assumption, the properties of air flow are calculated at the conditions of the dry air entering the system. It is assumed perfect mixture in the air, due to the fact that air has much higher rate than the candy flow and the operation experience.
- The external surface of each sphere is supposed to be surrounded by this cold air with constant properties. This assumption is based on the [0.5–3.0 m/s] range of air velocity (Zou et al., 2006).
- The convective heat-transfer coefficient is computed as the area averaged value of the local heat transfer coefficient (Becker and Fricke, 2004).

4.2. Heat transfer modeling

Based on the above assumptions, the energy balance of the unsteady heat transfer process in hard candies can be formulated as follows:

$$\frac{1}{\alpha_c}\frac{\partial T(r,t)}{\partial t} = \frac{\partial^2 T}{\partial r^2} + \frac{2}{r}\frac{\partial T}{\partial r} \qquad 0 < r < R \tag{1}$$

where (α) refers to the thermal diffusivity which is defined as follows:

$$\alpha = \frac{k_c}{\rho_c Cp_c} \tag{2}$$

where k_c, Cp_c and ρ_c refer, respectively, to the candy thermal conductivity, specific heat and density which are the most relevant model parameters for the analysis of food processes and process equipment design. Thermal diffusivity (α) defines how fast heat propagates or diffuses through a material (Singh, 1982), and it is generally affected by composition of the food product (Erdoğdu, 2008).

The boundary condition at the sphere surface ($r = R$) which is a third class condition is imposed by

$$k_c \frac{\partial T(r,t)}{\partial r} + h\ \ T(R,t) = h\ Ta_T, \quad r = R \tag{3}$$

where h and Ta_T refer respectively to the heat transfer coefficient and the cooling air temperature. As indicated in Eq. (3), the heat arriving at the sphere surface by conduction is dissipated into the medium by convection.

As regard the condition at the center $r = 0$, Eq. (4) refers to the adiabatic heat transfer condition by assuming that the product is evenly cooled

$$\frac{\partial T(r,t)}{\partial r} = 0\ r = 0 \tag{4}$$

Heat transfer coefficient (h) is computed by the correlation developed by Dincer (1994), which is applicable for air cooling of spherical and cylindrical products:

$$h = \frac{Nu\ k_a}{D_C} = (1.56\ \mathrm{Re}^{0.426}\ \mathrm{Pr}^{1/3})\frac{k_a}{D_c} \tag{5}$$

where k_a and D_c refer to the cooling air thermal conductivity and the candy diameter respectively. Nu is the Nusselt dimensionless Number.

Re and Pr are Reynolds and Prandtl dimensionless number respectively and are computed as follows:

$$Re = \frac{\rho_a v_a D_c}{\mu_a} \tag{6}$$

$$\mathrm{Pr} = \frac{Cp_a \mu_a}{k_a} \tag{7}$$

where ρ_a, v_a, μ_a, Cp_a and k_a are cooling air density, air velocity, specific heat and thermal conductivity respectively. D_c refers to the candy diameter.

Finally, a uniform initial temperature condition is considered as follows:

$$T(r,0) = T_{\mathrm{inl}} \quad 0 \leqslant r \leqslant R \tag{8}$$

where T_{inl} refers to the inlet candy temperature.

4.2.1. Discretization of the heat transfer modeling

Eqs. (1), (3), and (4) were discretized using the central finite difference method (CFDM). Fig. 4 schematically shows the boundary and internal nodes. The number of discretization points in time and radial direction have been chose equal to 11, defining:

$$\delta = \frac{R}{M}; \quad \Delta t = \frac{\theta}{N} \tag{9}$$

for the radial and temporal variations, respectively, with $M = N = 10$.

The second-order accurate in time and in space ($0[(\Delta t)^2,(\Delta x)^2]$) is the chosen method and is applied as follows:

First derivatives: the two-point formulae was used for internal nodes, that means i and/or $j \neq 0$, 10. The three-point formulae was applied for boundary nodes, i or $j = 0$ or 10. Three or four-point formulae were useful to compute the first derivative at a node on

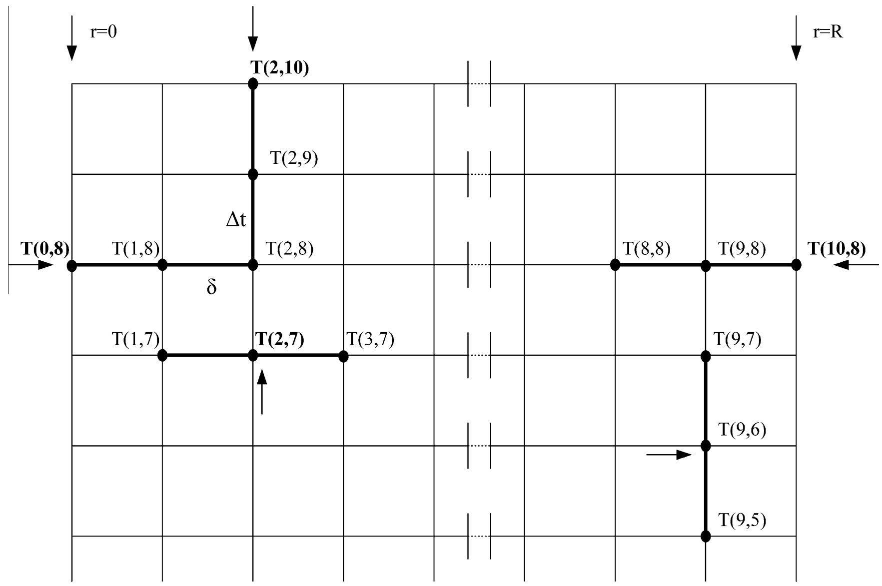

Fig. 4. Scheme of the discretization grid for CFDM.

the boundary by using more than two grid points on one side of the boundary in order to improve the accuracy of approximation (Ozisik, 1994).

Second derivatives: the *central* finite difference approximation is used at internal nodes (i and/or $j \neq 0$, 10), and the *forward* finite difference approximation is applied at the origin node, $i = 0$, at the boundary condition in the center of the sphere.

Thus, the following constraint computes the approximation of Eq. (1) for internal nodes:

$$\frac{T(i,j+1)-T(i,j-1)}{2\Delta t} = \alpha_c \frac{T(i-1,j)-2T(i,j)+T(i+1,j)}{\delta^2} + \frac{2}{(i-1)\delta}\left[\frac{T(i+1,j)-T(i-1,j)}{2\delta}\right], \quad \mathrm{i}:1,2,\ ,9;\ \mathrm{j}:1,2,\ ,\ 9 \tag{10}$$

The following constraint computes the temperature variation of the internal nodes at final time:

$$\frac{T(i,j-2)-4T(i,j-1)+3T(i,j)}{2\Delta t} = \alpha_c \frac{T(i-1,j)-2T(i,j)+T(i+1,j)}{\delta^2} + \frac{2}{(i-1)\delta}\left[\frac{T(i+1,j)-T(i-1,j)}{2\delta}\right], \quad i:1,2,\ldots,9; j:10 \tag{11}$$

The following are the constraints related to the discretizations of Eq. (3) and (4) which are the boundary conditions at the surface and center, respectively:

$$k_c \frac{T(i-2,j)-4T(i-1,j)+3T(i,j)}{2\delta} + h\,T(i,j) = h\,Ta\,, \quad i:10\,;\ j:1,\ 2,\ \ldots,\ 10 \tag{12}$$

$$\frac{T(i,j+1)-T(i,j-1)}{2\Delta t} = \alpha_c \frac{T(i-1,j)-2T(i,j)+T(i+1,j)}{\delta^2}, \quad i:0;\ j:1,2,\ldots,10 \tag{13}$$

The initial condition is imposed by:

$$T(i,j) = 80, \quad i:0,1,2\ldots,10;\ j:0 \tag{14}$$

The following constraint is imposed in order to ensure the glassy structure as well as to prevent quality problems (stickiness and deformation):

$$T(i,j) \leqslant 34, \quad i:0;\ j:10 \tag{15}$$

4.3. Modeling of the air aconditioning process

Mass and energy balances in mixer [M2]:

$$G_2 = G_1 + \mathrm{Rec} \tag{16}$$

$$G_2 H_2 = G_1 H_1 + \mathrm{Rec}\ H_{\mathrm{Rec}} \tag{17}$$

Mass balance in the Splitter [S]:

$$\mathrm{Rec} = Y G_2 \tag{18}$$

The cooling air flow-rate is computed according to the duct section [S], air density [ρ_a] and air linear velocity [v_a]:

$$G_2 = \rho_a \cdot v_a \cdot S \tag{19}$$

The heat transfer rate [q] in the heat exchanger [HE] is computed as follows:

$$q = U \cdot A \cdot \Delta T_{\mathrm{lm}} \tag{20}$$

where q and ΔT_{lm} refer to the transferred heat and logarithmic mean temperature difference, respectively.

Depending on the ambient air temperature (T_{amb}) the following constraints are imposed to compute both energy balance and ΔT_{lm} in the heat exchanger [HE]:

$$q = G_2 \cdot Cp_a \cdot (T_{HE}^{out} - T_{HE}^{inl}) = L_W \cdot Cp_W \cdot (T_L^{inl} - T_L^{out}), \qquad \text{if } Ta_T > T_{amb} \tag{21}$$

$$q = G_2 \cdot Cp_a \cdot (T_{HE}^{out} - T_{HE}^{inl}) = L_{CW} \cdot Cp_W \cdot (T_{CW} - T_L^{out}), \qquad \text{if } Ta_T < T_{amb} \tag{22}$$

$$\Delta T_{lm} = \frac{(T_L^{inl} - T_{HE}^{out}) - (T_L^{out} - T_{HE}^{inl})}{\ln \frac{(T_L^{inl} - T_{HE}^{out})}{(T_L^{out} - T_{HE}^{inl})}}, \qquad \text{if } Ta_T > T_{amb} \tag{23}$$

$$\Delta T_{lm} = \frac{(T_{HE}^{out} - T_{CW}) - (T_{HE}^{inl} - T_L^{out})}{\ln \frac{(T_{HE}^{out} - T_{CW})}{(T_{HE}^{inl} - T_L^{iout})}}, \qquad \text{if } Ta_T < T_{amb} \tag{24}$$

Eqs. (25) and (26) refer to the mass and energy balances in the Mixer M1:

$$L_W = L_{HW} + L_{CW} \tag{25}$$

$$H_W \cdot L_W = H_{HW} \cdot L_{HW} + H_{CW} \cdot L_{CW} \tag{26}$$

4.4. Connectivity constraints

According to Fig. 3, the following constraints are necessary to include in the model:

$$Ta_T^{inl} = Ta_T^{out} = T_{\text{Rec}} = Ta_T \tag{27}$$

4.5. Objective functions

One of the goals of the paper is to identify which objective function could be used to determine the operating conditions which lead to lower and more uniform temperature differences between the center and surface of the candy along the cooling tunnel. Based in previous and preliminary results about the influence of some variables on the cooling performance (Reinheimer, 2011; Reinheimer et al., 2010), some of the main model variables are included in the objective functions in order to investigate how the main model variables can be related among them in order to obtain an uniform temperature distribution during the cooling process. More precisely, the variables to be considered are: ΔT = the temperature difference between the center and surface of candy, Ta_T = air cooling temperature and v_a = air cooling velocity.

The following knowledge are considered to derive the three objective functions:

- Deformation, stickiness and rupture (fragility) are proportional to ΔT, so product quality increases with the decreasing of ΔT.
- The boundary condition at the sphere surface ($r = R$); Eq. (3) takes into account the heat transfer by convection between the surface of the candy and the medium and is strongly influenced by Ta_T and v_a. The rate of heat transfer by convection increases with the decreasing of Ta_T because the driving force between the candy and the medium increases. However, lower values of Ta_T lead to non-uniform temperature differences in the candy (ΔT).

The same rationale could be applied to explain the influence of the value of v_a on the heat transfer by convection. Higher values of v_a increase the heat transfer coefficient and therefore the rate of heat transfer. But also higher values of v_a cause temperature differences in the candy (ΔT).

According to this, there exists a trade-off of the value of Ta_T and v_a that should guarantee the cooling with more uniform temperature differences. Eq. (16) is imposed in the model to ensure the desired glassy structure.

Based on the mentioned above, the following three objective functions are investigated.

The first objective function OF1 consists of minimizing the ratio between ΔT at each time and Ta_T.

$$Min\ OF1 = Min\left[\frac{\sum_{j=0}^{10}[T(i=0,j) - T(i=10,j)]}{Ta_T}\right] \tag{28}$$

The authors believed that the minimization of the sum of ΔT at each instant of time leads to an uniform temperature difference in the candy; then it was considered in the numerator of OF1. As mentioned earlier, higher values of Ta_T lead to a more uniform ΔT than lower values. For this reason, Ta_T appears in the denominator of OF1.

Based on the same idea of OF1, the following objective function OF2 has been proposed. As shown, ΔT is only computed at the final time.

$$Min\ OF2 = Min\left[\frac{[T(i=0,j=10) - T(i=10,j=10)]}{Ta_T}\right] \tag{29}$$

OF2 was proposed to in order to compare the numerical results and computational cost (CPU time and iteration number) with that obtained by OF1.

Finally, OF3 only involves the main operating variables of the cooling tunnel. The idea behind is to verify if the minimization of the ratio between v_a and Ta_T, defined from the behaviors mentioned above, can guarantee a uniform temperature difference. Thus, the following objective function is also investigated:

$$Min\ OF3 = Min\left[\frac{v_a}{Ta_T}\right] \tag{30}$$

The model also includes constraints to compute enthalpies and air physical properties which are listed in Appendix A. Thus, Eqs. (9)–(26) are basically the model constraints that approximate the transient behavior of the cooling of the candy and the air conditioning process.

Briefly, the following three optimizations problems are stated:

- min OF1 (v_a, Ta_T, G_1, G_2, Y, L_{HW} if $Ta_T > T_{amb}$, or L_{CW} if $Ta_T < T_{amb}$); subject to Eqs. (9)–(26)
- min OF2 (v_a, T_{aT}, G_1, G_2, Y, L_{HW} if $T_{aT} > T_{amb}$, or L_{CW} if $T_{aT} < T_{amb}$); subject to Eqs. (9)–(26)
- min OF3 (v_a, Ta_T, G_1, G_2, Y, L_{HW} if $Ta_T > T_{amb}$, or L_{CW} if $Ta_T < T_{amb}$); subject to Eqs. (9)–(26)

As shown, the optimization variables are: v_a, Ta_T, G_1, G_2, Y and L_{HW} or L_{CW} depending on the specific study case.

The generalized reduced gradient algorithm CONOPT 2.041 was here used as NLP solver (Drud, 1992).

The optimization model involves, respectively, 170 and 80 equality and inequality constraints. The total number of variables is 176. It should be noticed that global optimal solutions cannot be guaranteed due to the presence of bilinear terms and logarithms which lead to non-convex constraints.

Intel Core i5 M480 2.67 GHz processor and 8 GB RAM has been used to perform the simulations and optimizations.

5. Experimental

Due to the layout design of the cooling tunnel, dynamic experimental data were not available for a rigorous model validation. It was no possible to install thermocouples within the candy, which is moving along the three cooling conveyor belts. Hence, in order to check the validity of the model, candy samples were taken at the end of the tunnel. Then, temperatures measured in the candy center and surface have been compared to those obtained by simulations. Experimental measurements were done by using a thermocouple type K (−50 to 350 °C) with TESTO 905-T1 (Testo) device with ±1 °C accuracy.

Several samples (n = 40) were taken at the outlet of the tunnel for each cooling experiment and rapidly placed in an insulated chamber. Temperatures on the surface and in the center of each candy were measured. A thermocouple was inserted into samples 8 mm below the surface to measure the temperature in the center. Then, every reading was recorded once the temperature has reached equilibrium. Experimental temperatures were reported as average values and standard deviation (Reinheimer et al., 2010).

6. Results and discussion

In this section, the validation of the proposed model and optimization results are presented through three case studies. The first case study deals with the model validation. The second one discusses the optimal results obtained for different objective functions. Finally, a sensitivity analysis is discussed in the case study 3.

6.1. Case study 1: Model validation

An exhaustive validation of the heat transfer model was presented in a previous work (Reinheimer et al., 2010). In that work, comparisons of the experimental and simulated temperatures obtained at the tunnel's outlet for different operating conditions and water contents showed slight differences on numerical values. Same conclusions were drawn for other size and chemical composition of hard candies.

Only for validation purpose, in this work, the model implemented in GAMS was used as a simulator in a predictive manner. For this, it was necessary to fix the model degree-of-freedom. Simulation results obtained by the actual model were compared with the experimental data used in Reinheimer et al. (2010). It is worth noting that both implemented models showed the same performance and results as expected.

After model validation, two study cases are presented in order to discuss the obtained results for the optimization problem described in Section 3.

6.2. Case study II: Optimal operating conditions of cooling tunnel for different optimization criteria

As mentioned, several objective functions based on different criteria have been investigated.

The model parameter values used for model optimization are listed in Table 1.

Lower and upper bounds in some optimization variables are listed in Table 2. For example, the air convection is directed by a horizontal fan with a safe operating speed range of 1.2–3 m/s, which is imposed by lower and upper bounds.

Table 1
Model parameter values.

Parameter	Value
Hard candy composition [w/w%]:	0.276
Carbohydrates	97.13
Water	2.5
Ash	0.18
Hard candy thermal conductivity, k_c [W/m °C]	0.276
Hard candy thermal diffusivity, α_c [m^2/s]	1.106E−7
Hard candy radio, R [m]	0.008
Air duct cross section, S [m^2]	0.2025
Specific heat capacity of water, Cp_W [J/kg °C]	4180
Specific heat capacity of air, Cp_a [J/kg °C]	1005
Overall heat transfer coefficient, U [W/m^2 °C]	200
Heat transfer area, A [m^2]	2.9
Ambient air temperature, T_{amb} [°C]	20
Ambient air relative humidity, RH [%]	46.5
Temperature of cold water utility, T_{CW} [°C]	25
Temperature of hot water utility, T_{HW} [°C]	50

Table 2
Lower and upper bounds for the main optimization variables.

Variable	Lower bound	Upper bound
Cooling air velocity, v_a [m/s]	1.2	3
Recycle ratio, Y	0	1

In order to analyze the optimal solutions it is important to keep in mind that the final temperature is critical for the wrapping session while the temperature difference between the surface and the center in each instant of time is crucial to avoid a sharp cooling which leads to serious quality problems (stickiness and deformation).

Figs. 5 and 6 compare, respectively, the corresponding temperature difference at each instance of time and the temperature profiles at the center and surface of the candy. For each objective function the comparison also includes results for two working modes of the cooling tunnel: (a) the cooling tunnel coupled to the air conditioning process (Examples 1, 3 and 5) and (b) the tunnel non coupled to the conditioning process (Examples 2 and 4). Despite that a maximum residence time of 500 s has been used to illustrate the obtained results, temperature profiles analysis for shorter residence times can be directly done from the presented figures.

A detailed comparison of solutions obtained for the three objective functions is also presented in Table 3.

As it can be clearly seen from Fig. 5, the risk of product fragility predicted by all objective functions is high at the beginning of the cooling process because the temperature differences reach the maximum values and then they decrease slowly down. As shown in Fig. 5, OF3 is the appropriate objective function in order to minimize the risk of product fragility. In contrast to our expectation, OF1 does not lead to minimize the risk of product fragility at each time during cooling. In fact, despite that OF1 leads to the minimum

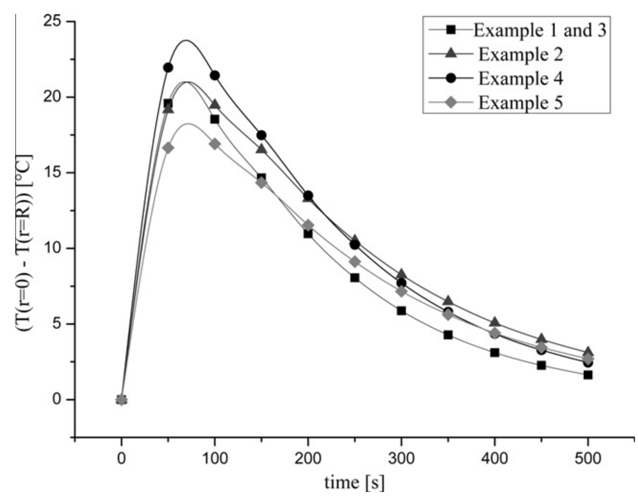

Fig. 5. Temperature difference vs. residence time.

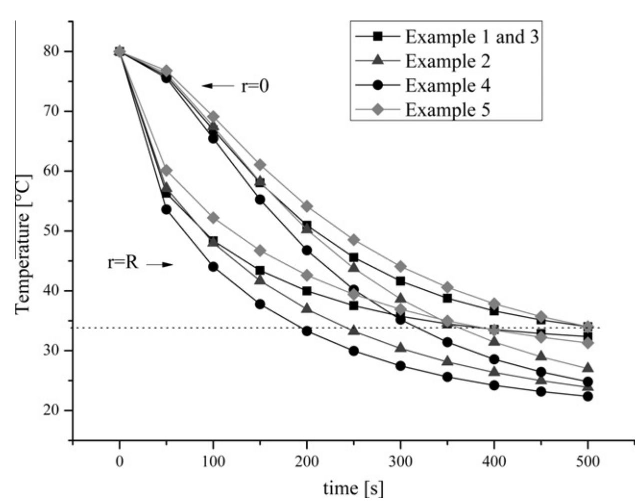

Fig. 6. Temperature profiles vs. residence time.

Table 3
Optimal values for different objective functions.

	OF1		OF2		OF3
	Example 1	Example 2	Example 3	Example 4	Example 5
v_a [m/s]	3 *	1.2 **	3 *	2.043	1.2 **
Ta_T [°C]	31.05	20.00	31.05	20.00	27.92
T_{HE}^{inl} [°C]	28.50	20.00	27.36	20.00	22.79
T_L^{inl} [°C]	34.44	N/A	35.80	N/A	30.64
T_L^{out} [°C]	31.69	N/A	32.09	N/A	25.50
ΔT_{lm} [°C]	3.287	N/A	4.739	N/A	2.714
G_1 [kg/s]	0.169	0.271	0.245	0.461	0.190
Rec [kg/s]	0.563	0.022	0.488	0.038	0.103
Y	0.769	0.076	0.666	0.076	0.352
G_2 [kg/s]	0.732	0.293	0.732	0.499	0.293
L_{HW} [kg/s]	0.062	N/A	0.076	N/A	0.016
L_{CW} [kg/s]	0.102	N/A	0.100	N/A	0.054
L_W [kg/s]	0.164	N/A	0.176	N/A	0.07
q [W]	1877.17	N/A	2719.98	N/A	1510.93
OF_1	3.051	5.543	3.051	5.716	3.446
OF_2	0.053	0.156	0.053	0.123	0.097
OF_3	0.097	0.06	0.097	0.102	0.043
Θ_{MIN} ($T_{r=0}$ = 34 °C) [s]	500	360	500	310	500
Sum ΔT [°C]	94.754	110.854	94.754	114.326	96.228

* Upper bound.
** Lower bound.

value of the sum of ΔT in each instance of time, the values of ΔT for OF1 at the beginning of the cooling are higher than values predicted by OF3. Based on this behavior, another objective function for minimization was investigated. It involves the sum of ΔT for the first points ranged between 0 and 150 s. As expected, this new objective function leads to the same solutions obtained by OF3.

Fig. 6 illustrates optimal temperature profiles indicating the minimum residence time for each objective function in order to reach the maximum admissible temperature at the end of the cooling tunnel (⩽34 °C). It can be clearly seen that all objective functions predicted the same minimum residence time (500 s.) when the cooling tunnel is coupled to air conditioning process.

In Examples 1, 3 and 5, the same minimum residence time is predicted, that means the glassy structure is reached at 500 s in the whole candy sample, being the temperature at its center equal to 34 °C. As shown in Table 3, this constraint is achieved by combination of two different pair of values of Ta_T and v_a.

In the specific cases of the applications of OF1 and OF3, there are no constraints on the value of v_a. Therefore, this variable adopts its upper bound. Due to the fact that v_a is high, the optimal value of Ta_T has to be high to minimize temperature differences, not to produce sharp cooling, and also because the ratio of these variables is involved in the minimization of the OF1 and OF2.

On the other hand, in the case of example 5, the minimization of the OF3 implicates the minimization of v_a, adopting its lower bound as optimal value. Consequently, the optimal value of Ta_T needs to be lower to contribute in the driving force for the heat transfer operation and therefore to assure the glassy structure imposed by the restriction.

Here, it is important to highlight that it is assumed that the necessary utilities to heat the cooling temperature and provide the power for the horizontal fan, are enough. Both can be supplied without restrictions.

The residence time is an important process parameter because it is strongly connected with the candy production level, operating costs as well as the operating mode of the cooling tunnel. For example, for a fixed tunnel dimensions, higher residence time results in smaller production.

According to Table 3, in all cases except for Example 4, v_a reached its bounds; more precisely upper bound in Examples 1 and 3 and lower bound in Examples 2 and 5.

Because the optimal value of Ta_T using OF3 is 27.92 °C instead of 31.05 °C and the cooling air velocity is 1.2 m/s instead of 3 m/s, the estimated values of the heat transfer duty on the exchanger as well as the flow-rate of the stream used for heating predicted by OF3 are smaller than those predicted by OF1 and OF2 (24.23% and 80.02% for heat duty and 134.28% and 151.42% for flow-rate of hot stream, respectively). In addition, the quantity of air recycled using OF3 is considerably lower than using OF1 and OF2. These results clearly show the sensitivity of the operating variables (stream temperatures and flow rates) on the objective functions. However, it should be mentioned that the results were obtained neglecting the air pressure drop along the heat exchanger and the cooling tunnel. For a more accuracy, the dependence of the heat transfer coefficients with the temperature, fluid velocities as well as the air pressure drop should be considered.

6.3. Case study III

In order to investigate the effect of the ambient air temperature (T_{amb}) on the whole cooling process (cooling tunnel plus air conditioning process), the optimization model was also solved for different ambient air temperature values. Table 4 reports the results obtained for T_{amb} = 15, 20, 25 and 30 °C and considering OF3. As shown in Table 4, same optimal values of v_a (1.2 m/s) and Ta_T (27.92 °C) are reached for all T_{amb} values remarking that v_a reached its lower bound. A same optimal temperature value was achieved because it was assumed in all cases that enough hot and cold utilities are available. In fact, both recycle of heated air and hot stream were used to heat the incoming air stream for $T_{amb} < Ta_{T(\text{optimal})}$ and cold stream to cool incoming air for $T_{amb} \geqslant Ta_{T(\text{optimal})}$.

As expected, it is clearly observed that the transferred heat [q] in the heat exchanger increases as T_{amb} decreases for T_{amb}. Also, it is possible to conclude that the air recycled [Rec] increases its rate with the decreasing of the T_{amb} value.

The fourth column in Table 4 shows the results obtained for T_{amb} = 30 °C (T_{amb} > optimal Ta_T). In this case, the optimal values corresponding for Ta_T and v_a also are 27.92 °C and 1.2 m/s, respectively. Thus, 0.012 kg/s of cold stream (L_{CW}) is used to cool the incoming air stream using a fixed heat transfer area of 2.9 m^2.

From the obtained results, a sensitivity analysis indicates that the optimal value will improve as v_a decreases because it reached its lower bound. However, it is not technologically feasible to operate the tunnel at lower air velocity than 1.2 m/s.

6.4. Sensitivity analysis with respect to radial discretization

In order to study the influence of the number of discretization grid points used on the numerical results, a sensitivity analysis was conducted. The obtained results showed that numerical results are not affected when the number of discretization grid points used is higher than 10. Certainly, despite that the computing time and the number of iterations increased slightly when the number of grid points was higher than 10, same numerical values were found when the number of discretization grid points was higher than 10. However, poor results have been obtained when the number of grid points was smaller than 10. In fact, inaccurate temperature transients were predicted. Thus, according to the accuracy of results, computational time and number of iterations, 10 nodes were selected for the discretization purpose.

6.5. Computational aspects

It is interesting to mention some details about the initialization of all model variables. In order to obtain a feasible initial solution to guarantee the convergence of the proposed optimization NLP model the following initialization strategy has been successfully

Table 4
Optimal values obtained using OF3 for different T_{amb}.

	Average ambient air temperature (T_{amb})			
	15 °C	20 °C	25 °C	30 °C
v_a [m/s]	1.2 **	1.2 **	1.2 **	1.2 **
Ta_T [°C]	27.29	27.29	27.29	27.29
T_{HE}^{inl}[°C]	22.31	22.79	25.25	29.91
T_L^{inl}[°C]	30.89	30.64	29.57	25.00
T_L^{out}[°C]	25.27	25.50	26.45	29.69
ΔT_{lm} [°C]	2.968	2.714	1.412	1.052
G_1 [kg/s]	0.127	0.190	0.267	0.281
Rec [kg/s]	0.166	0.103	0.029	0.012
Y	0.566	0.352	0.087	0.42
G_2 [kg/s]	0.293	0.293	0.293	0.293
L_{HW} [kg/s]	0.017	0.016	0.011	N/A
L_{CH} [kg/s]	0.054	0.054	0.049	0.012
L_W [kg/s]	0.071	0.07	0.060	N/A
q [W]	1652.75	1510.93	786.04	585.49

** Lower bound.

implemented. In a first step, the optimization variables are fixed at known values and thus the NLP model becomes into a linear programing model (LP) and is solved in a simulation mode. The main advantage of this is that LP models are more easy to solve than NLP models because they are not strongly dependent on the initial values. Then, in a second step, the values that were previously fixed are now set as free values and the solution obtained by the LP model (simulation mode) is used as initialization to solve the NLP optimization model. Both steps were implemented in a systematic way and external input data are not required. Thus, initial values for all model variables were automatically obtained in a few iterations. In addition, several tests using different random initialization settings have been also considered. In some cases, same solutions reported in the paper have been obtained but in other cases, the optimization algorithm failed.

However, despite that same solutions were obtained in some of the cases, global solutions cannot be guaranteed due to the non-convex constraints involved in the mathematical model.

Finally, it should be mentioned that scaling on variables and equations has been also implemented in order to facilitate the model convergence. Thus, the proposed problems were solved at a relatively low computational cost. Certainly, all solutions were obtained rapidly in at worst 0.12 CPU seconds after 12 iterations. The model proved to be robust and flexible, achieving convergence in all the several optimization made.

7. Conclusions

A mathematical model for predicting the temperature variation in hard candies during cooling was presented. The proposed model allows to determine the optimal operating conditions of the cooling tunnel and the air conditioning process in order to maximize the product quality. A centered finite difference approximation (CFDM) was used to discretize the PDAEs into a set of non linear algebraic equations.

Three formulations of objective functions considering quality aspects implicitly were investigated. Same behaviors of hard candy temperature profiles have been predicted by all objective functions, indicating that the risk of product fragility is high at the beginning of the cooling.

Contrary to our expectation, numerical results showed that OF3 predicts lower temperature differences than OF1 and OF2. From quality aspect, this result is valuable because it indicates that it is preferred to include the operating variables of the cooling tunnel in the objective function instead of temperature differences. Regardless of this, it is also interesting to observe that the minimization of the temperature difference at the beginning of the cooling (first instances of time), leads to the same solutions predicted by OF3. It is important to remark here, that heterogeneous temperature distributions will always exist due to the high internal heat transfer resistance (low value of thermal conductivity) of hard candies.

The results discussed in this paper were obtained for a cooling tunnel composed of three conveyor belts assuming a same velocity for each one of them. It may be possible, however, to operate the conveyor belts at different velocities if the cooling efficiency is improved. The convenience of such modifications can be analyzed by extending the presented model in order to consider different velocities for the conveyor belts. Moreover, the production level, the total cost and quality models must be also considered for the optimization. Certainly, many other optimization problems can be stated if the mentioned aspects are considered to be part of the trade-offs. For example, the following optimization problems could be set: (i) to minimize residence time and minimize temperature differences, (ii) to minimize residence time given a constraint of maximum temperature difference smaller than a certain value. Thus, all trade-offs given by quality and economic aspects can be simultaneous optimized. These mentioned aspects will be addressed in future studies. In this sense, the results discussed in this paper are valuable and useful because they can be further used to explore other optimization problems. For example, the minimum values reported of the maximum temperature differences observed in the cooling tunnel, which are related to the product quality, can be further imposed as a model constraint. The main advantage of this is that quality aspects can be handled by constraints and thus other aspects can be explicitly included in the objective functions.

According to the above findings, it is easy to conclude that an economic objective function including operating costs and investment must be considered for the design of the air conditioning process. Operating costs for heating are given by the electricity consumed by the air blower used for recycling of heated air [Rec] and pumps used for the hot water [HW] stream. And the investment costs are related to the air cooling tower, blowers and pumps.

Acknowledgment

The authors greatly acknowledge the Consejo Nacional de Investigaciones Científicas y Técnicas (CONICET) and the Universidad Tecnológica Nacional Facultad Regional Rosario (UTN-FRRo) for its financial supports.

Appendix A

The enthalpies used in the energy balances are computed as follows:

$$H_2 = Cp_a \cdot (Ta_{HE}^{inl} - T_{ref}) \quad (31)$$

$$H_1 = Cp_a \cdot (Ta_{amb} - T_{ref}) \quad (32)$$

$$H_{\mathrm{Rec}} = Cp_a \cdot (Ta_T^{out} - T_{ref}) \quad (33)$$

$$H_W = Cp_W \cdot (T_L^{inl} - T_{ref}) \quad (34)$$

$$H_{HW} = Cp_W \cdot (T_{HW} - T_{ref}) \quad (35)$$

$$H_{CW} = Cp_W \cdot (T_{CW} - T_{ref}) \quad (36)$$

Correlations for the calculation of the cooling air thermophysical properties (Tsilingiris, 2008):

$$\rho_a = 1.293393662 - 5.538444326\mathrm{E}-3 \cdot Ta_T + 3.860201577\mathrm{E}-5 \cdot Ta_T^2 - 5.2536065\mathrm{E}-7 \cdot Ta_T^3 \quad (37)$$

$$k_a = 2.40073953E-2 + 7.278410162E-5 \cdot Ta_T - 1.788037411E-7 \cdot Ta_T^2 - 1.351703529E-9 \cdot Ta_T^3 - 3.322412767E-11 \cdot Ta_T^4 \quad (38)$$

$$\mathrm{Pr_a} = 0.7215798365 - 3.703124976E-4 \cdot Ta_T + 2.240599044E-5 \cdot Ta_T^2 - 4.162785412E-7 \cdot Ta_T^3 + 4.969218948E-9 \cdot Ta_T^4 \quad (39)$$

$$\mu_a = 1.715747771E-5 + 4.722402075E-8 \cdot Ta_T - 3.663027156E-10 \cdot Ta_T^2 + 1.873236686E-12 \cdot Ta_T^3 - 8.050218737E-14 \cdot Ta_T^4 \quad (40)$$

References

Balsa-Canto, E., Banga, J.R., Alonso, A.A., 2002. A novel efficient and reliable method for thermal process design and optimization. Part I: theory. Journal of Food Engineering 52 (3), 227–234.

Banga, J.R., Balsa-Canto, E., Moles, C.G., Alonso, A.A., 2003. Improving food processing using modern optimization methods. Trends in Food Science and Technology 14 (4), 131–144.

Barttfeld, M., Alleborn, N., Durst, F., 2006. Dynamic optimization of multiple-zone air impingement drying processes. Computers and Chemical Engineering 30, 467–489.

Becker, B.R., Fricke, B.A., 2004. Heat transfer coefficients for forced air cooling and freezing of selected foods. International Journal of Refrigeration 27, 540–551.

Bouraoui, M.M., Fichtali, J., Arteaga, G., Nakai, S., 1998. Optimization of the setting and cooking conditions for making gels from Pacific Whiting Surimi. Journal of Food Processing and Preservation 22, 169–184.

Box, G.E.P., Hunter, W.G., Hunter, J.S., 1978. Statistics for Experimenters: an Introduction to Design, Data Analysis and Model Building. John Wiley and Sons, New York USA.

Choi, Y., Okos, M., 1986. Effects of temperature and composition on the thermal properties of foods. Food Engineering and Process Application 1, 93–116.

Dincer, I., 1994. Development of new effective Nusselt–Reynolds correlations for air–cooling of spherical and cylindrical products. International Journal of Heat and Mass Transfer 37, 2781–2787.

Drud, A., 1992. CONOPT-A large scale GRG code. ORSA Journal on Computing 6, 207–216.

Erbar, Z., Icier, F., 2009. Optimization of hot air drying of olive leaves using response surface methodology. Journal of Food Engineering 91, 533–541.

Erdoğdu, F., 2008. A review on simultaneous determination of thermal diffusivity and heat transfer coefficient. Journal Food Engineering 86, 453–459.

Espinoza-Pérez, J.D., Vargas, A., Robles-Olvera, V.J., Rodríguez-Jimenes, G.C., García-Alvarado, M.A., 2007. Mathematical modeling of caffeine kinetic during solid-liquid extraction of coffee beans. Journal of Food Engineering 81, 72–78.

Firatligil-Durmus, E., Evranuz, O., 2010. Response surface methodology for protein extraction optimization of red pepper seed. LWT-Food Science and Technology 43, 226–231.

Kiziltaş, S., Erdoğdu, F., Palazoğlu, T.K., 2010. Simulation of heat transfer for solid-liquid food mixtures in cans and model validation under pasteurization conditions. Journal Food Engineering 97 (4), 449–456.

Myers, R., Montgomery, D., 2002. Response Surface Methodology: Process and Product Optimization using Designed Experiments, second ed. John Wiley and Sons Inc, New York USA.

Norton, T., Delgado, A., Hogan, E., Grace, P., Sun, D.-W., 2009. Simulation of high pressure freezing processes by enthalpy method. Journal Food Engineering 91 (2), 260–268.

Nowee, S.M., Abbas, A., Romagnoli, J.A., 2007. Optimization in seeded cooling crystallization: a parameter estimation and dynamic optimization study. Chemical Engineering and Processing 46, 1096–1106.

Ozisik, M.N., 1994. Finite Difference Methods in Heat Transfer. CRC Press, Boca Raton, Florida.

Purlis, E., 2011. Bread baking: technological considerations based on process modeling and simulation. Journal of Food Engineering 103 (1), 92–102.

Reinheimer, M.A., Mussati, S., Scenna, N.J., 2010. Influence of product composition and operation conditions on the unsteady behavior of hard candy cooling process. Journal of Food Engineering 101 (4), 409–416.

Reinheimer, M.A. (2011). Diseño Conceptual de procesos en Ingeniería de Alimentos. Incorporación de la microestructura en el análisis. PhD Thesis. Universidad Nacional del Litoral, Facultad de Ingeniería Química. Santa Fe, Argentina.

Singh, R., 1982. Thermal diffusivity in food processing. Food Technology 36, 87–91.

Tsilingiris, P.T., 2008. Thermophysical and transport properties of humid air at temperature range between 0 °C and 100 °C. Energy Conversion and Management 49 (5), 1098–1110.

Zou, Q., Opara, L.U., McKibbin, R., 2006. A CFD modeling system for airflow and heat transfer in ventilated packaging for fresh foods: I. Initial analysis and development of mathematical models. Journal of Food Engineering 77, 1037–1047.